https://doi.org/10.17952/37EPS.2024.P1160

Discovery of a novel α-helical peptide targeting GTP-bound K-Ras(G12D)

Hannah Comfort[1], Sarah Ross[2], Jefferson Revell[3], Thomas Murray[4], Carole Urbach[4], Bethan Archer[4], Darerca Owen[1] and Helen Mott[1]

[1]Department of Biochemistry, University of Cambridge, UK; [2]Oncology R&D, AstraZeneca, Cambridge, UK; [3]Discovery Sciences, AstraZeneca R&D, Cambridge, UK; [4]Biologics Engineering, AstraZeneca R&D, Cambridge, UK

1. Introduction

- K-Ras inhibition has been a major goal of cancer drug discovery for decades and there remain no clinically approved therapeutics directly targeting common K-Ras mutants such as G12D or G12V[1].
- Oncogenic K-Ras activates tumourigenic signalling pathways by binding to effector proteins, such as cRaf, in the GTP-bound form. Effector proteins bind predominately at the K-Ras switch regions, whose conformation is distinct in GTP- and GDP-bound K-Ras.
- Helical peptides can provide efficacious inhibitors of large protein-protein interfaces, such as that of K-Ras and its downstream effectors.
- A phage display screen of an α-helical peptide library identified a novel K-Ras(G12D) binder, which has been characterised biochemically and in a cellular context.

2. Biochemical characterisation of P39 binding

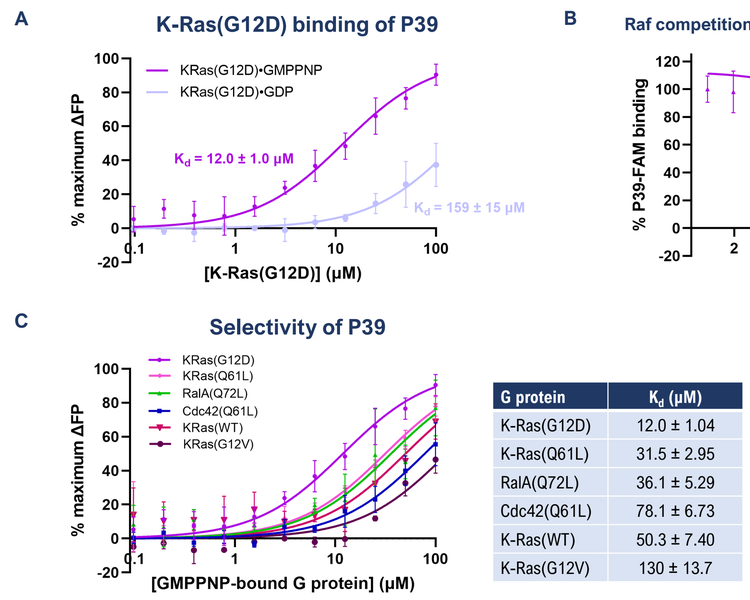

G protein	K_d (μM)
K-Ras(G12D)	12.0 ± 1.04
K-Ras(Q61L)	31.5 ± 2.95
RalA(Q72L)	36.1 ± 5.29
Cdc42(Q61L)	78.1 ± 6.73
K-Ras(WT)	50.3 ± 7.40
K-Ras(G12V)	130 ± 13.7

Figure 5. Characterisation of hit from naïve screen (P39)

(A) Fluorescence polarization (FP) of FAM-39 was measured with shown concentrations of GDP or GMPPNP-bound K-Ras(G12D). (B) FP was detected following addition of cRaf RBD to a complex of K-Ras(G12D)·GMPPNP and FAM-39. (C) FP of FAM-39 was measured with shown concentrations of various GMPPNP-bound G proteins.

A naïve screen of a helical peptide library against K-Ras(G12D) yielded numerous hits. Of these, P39 was selected for further characterisation and was found by FP to bind K-Ras(G12D) bound to the GTP analogue GMPPNP with >10-fold selectivity over the GDP-bound form (Figure 1A).

The K-Ras effector cRaf can also compete with P39 for K-Ras(G12D)·GMPPNP binding (Figure 1B), suggesting that the peptide may bind at the effector-binding interface.

Finally, P39 has some selectivity for K-Ras(G12D) binding over other G proteins as well as WT K-Ras and other common oncogenic mutants (Figure 1C).

3. NMR titration to map P39 binding site

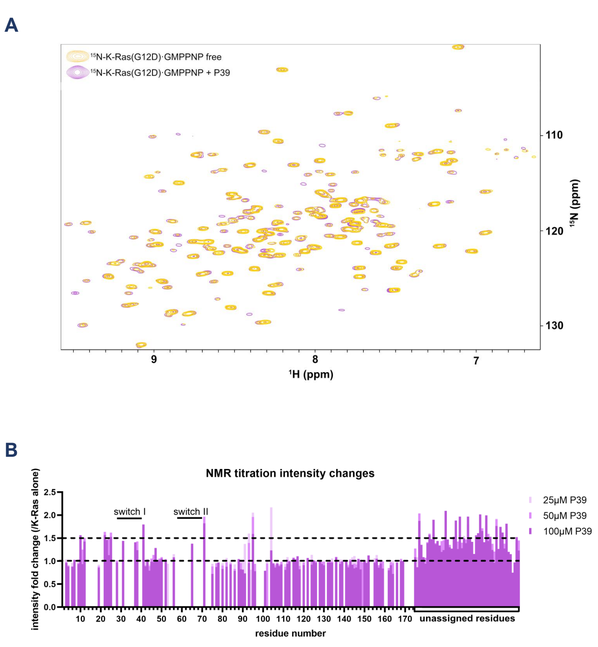

Figure 2. NMR titrations of P39 into 15N-K-Ras(G12D)·GMPPNP

(A) HSQC of ^{15}N-K-Ras(G12D)·GMPPNP was detected before (orange) and after (pink) addition of P39. (B) Intensity changes of peaks in ^{15}N-K-Ras(G12D)·GMPPNP HSQC upon addition of P39.

NMR was utilised to map the P39 binding site of K-Ras(G12D). Titration of P39 into ^{15}N-labelled K-Ras(G12D)·GMPPNP revealed an increase in intensity in numerous peaks in the HSQC spectrum (Figure 2A).

The residues for which peaks increased in intensity were found to be in or around the switch regions of K-Ras (Figure 2B). In addition, a number of new peaks appeared in the spectrum. These are likely to be within the switch regions, whose peaks are too weak to be assigned in free K-Ras.

This suggests that P39 likely binds to the switch I and switch II regions of K-Ras(G12D) and stabilises their conformation, increasing their HSQC peak intensity. K-Ras effector proteins also bind at the switch regions, consistent with the Raf-competitive binding of P39.

4. MD simulations of the P39-K-Ras(G12D) complex

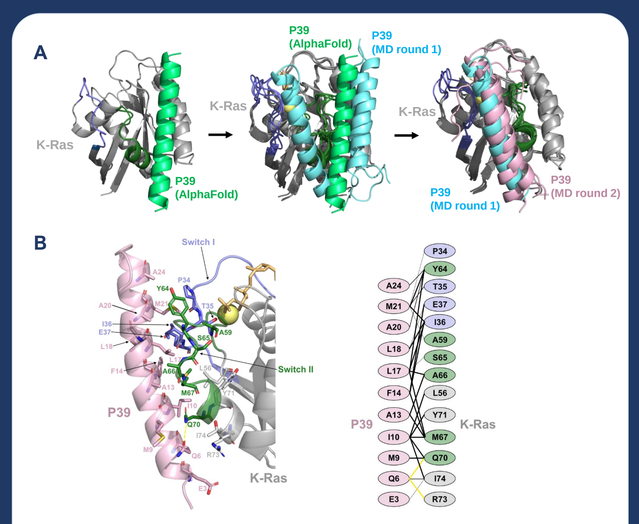

Figure 3. MD simulations of the P39-K-Ras(G12D) complex

(A) Starting from an AlphaFold model of the P39-K-Ras(G12D) complex a series of 300ns MD simulations revealed a stable binding site for P39. (B) Contacts between P39 and K-Ras(G12D)·GMPPNP over the simulation with the lowest P39 RMSD. Switch I is coloured blue, switch II is coloured dark green. Yellow line = polar contact.

Molecular dynamics (MD) simulations of an AlphaFold model of the P39-K-Ras(G12D) complex were used to predict the binding site of P39.

The initial three replicas differed, with one replica predicting a significant deviation from the AlphaFold model (Figure 3A center image). Performing three replica MD simulations from this starting point revealed a stable P39 binding pose between switch I and switch II (Figure 3A right image), supporting the NMR titration data.

Analysis of P39-K-Ras contacts reveals a largely hydrophobic interface (Figure 3B).

5. P39 interaction with K-Ras in HEK-293T cells

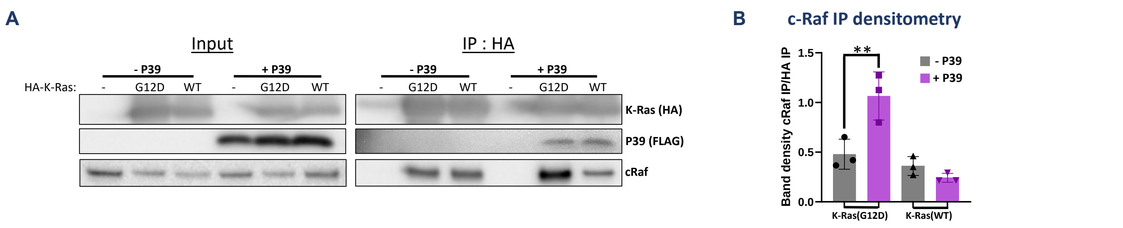

Figure 4. Co-immunoprecipitation of P39 with K-Ras when co-expressed in HEK-293T cells

(A) HA-K-Ras and P39-FLAG or empty vector were co-transfected into HEK-293T cells. HA-K-Ras was immunoprecipitated with anti-HA magnetic beads and associated proteins were identified by Western Blot. (B) Quantification of band intensity for cRaf from three independent co-immunoprecipitation experiments in HEK-293T cells co-transfected with K-Ras and P39 or empty vector. ** = 0.0021<p<0.033 by t-test.

To assess whether P39 interacts with K-Ras in a cellular context, HEK-293T cells were co-transfected with HA-tagged K-Ras(G12D) or K-Ras(WT) and FLAG-tagged P39 or an empty vector. K-Ras was immunoprecipitated and associated P39 was identified by Western Blot. P39 co-immunoprecipitated with both K-Ras(G12D) or K-Ras(WT) confirming the interaction (Figure 4A). The interaction between transfected HA-K-Ras and endogenous cRaf was also assessed, which surprisingly revealed an increase in the K-Ras(G12D)-cRaf interaction in the presence of P39 (Figure 4A/B).

6. Activity of P39 in KRAS(G12D)-mutant cells

To assess the effect of P39 on endogenous K-Ras(G12D) signalling, the KRAS(G12D)-mutant colon cancer cell line GP2D was utilised. P39 was appended with an octa-arginine sequence to enable cell penetration.

P39 treatment resulted in an increase in the K-Ras-Raf interaction in these cells (Figure 5A). This led to an increase in K-Ras signalling pathway markers in P39 treated cells, including MAPK pathway markers (pERK/pMEK) and PI3K pathway marker pAKT (Figure 5B). An increase in cleaved PARP was also seen indicating that Ras hyperactivity is driving apoptosis.

P39 did not increase Ras signalling or apoptosis in the K-Ras-independent BRAF(V600E)-mutant cell line HT29, indicating a specific response in the GP2Ds.

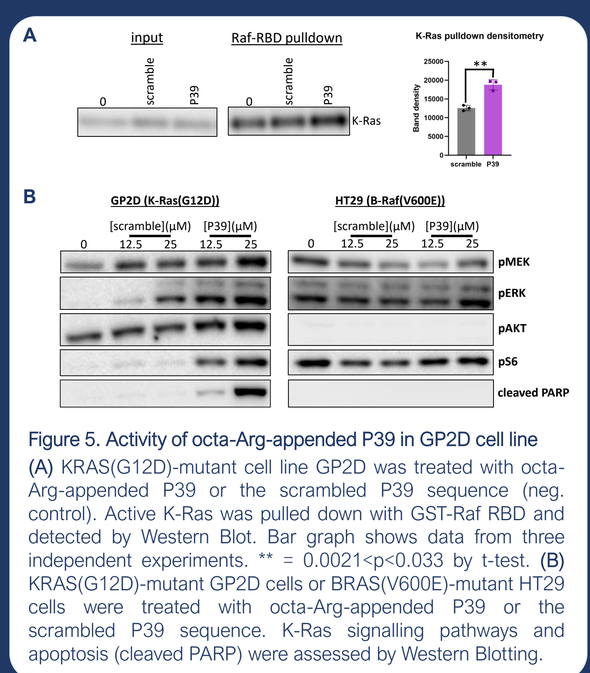

Figure 5. Activity of octa-Arg-appended P39 in GP2D cell line

(A) KRAS(G12D)-mutant cell line GP2D was treated with octa-Arg-appended P39 or the scrambled P39 sequence (neg. control). Active K-Ras was pulled down with GST-Raf RBD and detected by Western Blot. Bar graph shows data from three independent experiments. ** = 0.0021<p<0.033 by t-test. (B) KRAS(G12D)-mutant GP2D cells or BRAS(V600E)-mutant HT29 cells were treated with octa-Arg-appended P39 or the scrambled P39 sequence. K-Ras signalling pathways and apoptosis (cleaved PARP) were assessed by Western Blotting.

7. Conclusions

- A phage display screen of an α-helical peptide library against K-Ras(G12D) identified P39, which binds K-Ras(G12D) with **>10-fold selectivity for the active state**.
- P39 binding is somewhat selective for K-Ras over other G proteins (RalA and Cdc42) and for the G12D mutant over other K-Ras mutants (WT, Q61L and G12V).
- P39 is predicted to **bind between switch I and II** of K-Ras(G12D) through a largely hydrophobic interface.
- Octa-Arg-appended P39 **increases the K-Ras-Raf interaction in a KRAS(G12D)-mutant cancer cell line**, resulting in an increase in Ras signalling.
- Hyperactivation of Ras signalling by P39 **leads to apoptosis** in a KRAS(G12D)-mutant cancer cell line.

References

[1]Nussinov R and Jang H (2025) Direct K-Ras Inhibitors to Treat Cancers: Progress, New Insights, and Approaches to Treat Resistance. *Annu. Rev. Pharmacol.*

UNIVERSITY OF CAMBRIDGE

AstraZeneca